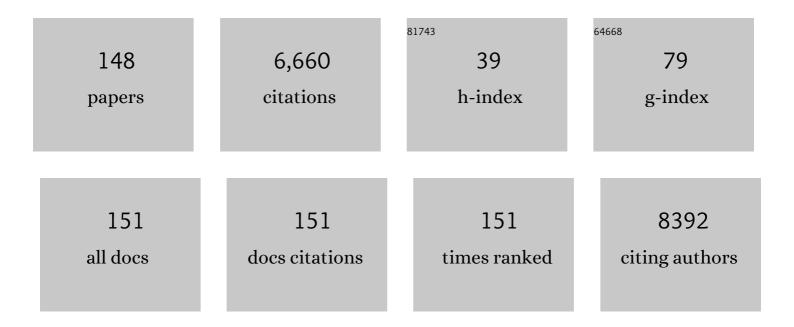
List of Publications by Year in descending order

Source: https://exaly.com/author-pdf/5477600/publications.pdf Version: 2024-02-01



Μινιορίι Οςλόλ

#	Article	lF	CITATIONS
1	Twoâ€Dimensional Dielectric Nanosheets: Novel Nanoelectronics From Nanocrystal Building Blocks. Advanced Materials, 2012, 24, 210-228.	11.1	987
2	Exfoliated oxide nanosheets: new solution to nanoelectronics. Journal of Materials Chemistry, 2009, 19, 2503.	6.7	543
3	Thermoresponsive actuation enabled by permittivity switching in an electrostatically anisotropic hydrogel. Nature Materials, 2015, 14, 1002-1007.	13.3	530
4	Large remanent polarization of (Bi,Nd)4Ti3O12 epitaxial thin films grown by metalorganic chemical vapor deposition. Applied Physics Letters, 2002, 80, 2746-2748.	1.5	348
5	Vapour–liquid–solid growth of monolayer MoS2 nanoribbons. Nature Materials, 2018, 17, 535-542.	13.3	286
6	High-κ Dielectric Nanofilms Fabricated from Titania Nanosheets. Advanced Materials, 2006, 18, 1023-1027.	11.1	206
7	Construction of Highly Ordered Lamellar Nanostructures through Langmuirâ^'Blodgett Deposition of Molecularly Thin Titania Nanosheets Tens of Micrometers Wide and Their Excellent Dielectric Properties. ACS Nano, 2009, 3, 1097-1106.	7.3	171
8	Effect of cosubstitution of La and V in Bi4Ti3O12 thin films on the low-temperature deposition. Applied Physics Letters, 2002, 80, 100-102.	1.5	169
9	Robust High-κ Response in Molecularly Thin Perovskite Nanosheets. ACS Nano, 2010, 4, 5225-5232.	7.3	141
10	Engineered Interfaces of Artificial Perovskite Oxide Superlattices <i>via</i> Nanosheet Deposition Process. ACS Nano, 2010, 4, 6673-6680.	7.3	141
11	Gigantic Magneto–Optical Effects in Multilayer Assemblies of Two-DimensionalÂTitania Nanosheets. Advanced Materials, 2006, 18, 295-299.	11.1	137
12	Large magnetoelectric coupling in magnetically short-range ordered Bi5Ti3FeO15 film. Scientific Reports, 2014, 4, 5255.	1.6	135
13	Chemical composition and crystal structure of superconducting sodium cobalt oxide bilayer-hydrateElectronic supplementary information (ESI) available: Rietveld refinement patterns. See http://www.rsc.org/suppdata/jm/b4/b400181h/. Journal of Materials Chemistry, 2004, 14, 1448.	6.7	117
14	Defect Engineering for Control of Polarization Properties in SrBi2Ta2O9. Japanese Journal of Applied Physics, 2002, 41, 7062-7075.	0.8	114
15	Preparation and characterization of a- and b-axis-oriented epitaxially grown Bi4Ti3O12-based thin films with long-range lattice matching. Applied Physics Letters, 2002, 81, 1660-1662.	1.5	101
16	Large remanent polarization of Bi4Ti3O12-based thin films modified by the site engineering technique. Journal of Applied Physics, 2002, 92, 1518-1521.	1.1	92
17	High performance silicon-based anodes in solid-state lithium batteries. Energy and Environmental Science, 2014, 7, 662-666.	15.6	84
18	All-Nanosheet Ultrathin Capacitors Assembled Layer-by-Layer <i>via</i> Solution-Based Processes. ACS Nano, 2014, 8, 2658-2666.	7.3	82

#	Article	IF	CITATIONS
19	<i>In Situ</i> Tuning of Magnetization and Magnetoresistance in Fe <sub>3</sub> O <sub>4</sub> Thin Film Achieved with All-Solid-State Redox Device. ACS Nano, 2016, 10, 1655-1661.	7.3	80
20	Wafer-scale and deterministic patterned growth of monolayer MoS <sub>2</sub> <i>via</i> vapor–liquid–solid method. Nanoscale, 2019, 11, 16122-16129.	2.8	76
21	Controlled Polarizability of Oneâ€Nanometerâ€Thick Oxide Nanosheets for Tailored, Highâ€≺i>κ Nanodielectrics. Advanced Functional Materials, 2011, 21, 3482-3487.	7.8	72
22	The rise of 2D dielectrics/ferroelectrics. APL Materials, 2019, 7, .	2.2	66
23	Graphitic Carbon Nitrideâ€Based Lowâ€Dimensional Heterostructures for Photocatalytic Applications. Solar Rrl, 2020, 4, 1900435.	3.1	65
24	Synthesis of Mn-Substituted Titania Nanosheets and Ferromagnetic Thin Films with Controlled Doping. Chemistry of Materials, 2009, 21, 4366-4373.	3.2	63
25	Neat monolayer tiling of molecularly thin two-dimensional materials in 1 min. Science Advances, 2017, 3, e1700414.	4.7	63
26	RbBiNb <sub>2</sub> O <sub>7</sub> : A New Lead-Free High- <i>T</i> <sub>c</sub> Ferroelectric. Chemistry of Materials, 2012, 24, 3111-3113.	3.2	60
27	Ferroelectric properties of lanthanide-substituted Bi4Ti3O12 epitaxial thin films grown by metalorganic chemical vapor deposition. Journal of Applied Physics, 2003, 93, 1707-1712.	1.1	55
28	Atomic Layer Engineering of High-κ Ferroelectricity in 2D Perovskites. Journal of the American Chemical Society, 2017, 139, 10868-10874.	6.6	55
29	The effects of oxygen partial pressure on local structural properties for Ga-doped ZnO thin films. Thin Solid Films, 2006, 494, 38-41.	0.8	53
30	2D Perovskite Nanosheets with Thermally-Stable High-κ Response: A New Platform for High-Temperature Capacitors. ACS Applied Materials & Interfaces, 2014, 6, 19510-19514.	4.0	50
31	High Thermal Robustness of Molecularly Thin Perovskite Nanosheets and Implications for Superior Dielectric Properties. ACS Nano, 2014, 8, 5449-5461.	7.3	49
32	Tunable Bandgap Narrowing Induced by Controlled Molecular Thickness in 2D Mica Nanosheets. Chemistry of Materials, 2015, 27, 4222-4228.	3.2	47
33	Gigantic magneto-optical effects induced by (Feâ^•Co)-cosubstitution in titania nanosheets. Applied Physics Letters, 2008, 92, 253110.	1.5	46
34	Selfâ€Assembly Atomic Stacking Transport Layer of 2D Layered Titania for Perovskite Solar Cells with Extended UV Stability. Advanced Energy Materials, 2018, 8, 1701722.	10.2	46
35	Coexistence of Magnetic Order and Ferroelectricity at 2D Nanosheet Interfaces. Journal of the American Chemical Society, 2016, 138, 7621-7625.	6.6	45
36	Orbital Reconstruction and Interface Ferromagnetism in Self-Assembled Nanosheet Superlattices. ACS Nano, 2011, 5, 6871-6879.	7.3	44

#	Article	IF	CITATIONS
37	Self-Assembled Nanofilm of Monodisperse Cobalt Hydroxide Hexagonal Platelets: Topotactic Conversion into Oxide and Resistive Switching. Chemistry of Materials, 2010, 22, 6341-6346.	3.2	42
38	Nanoarchitectonics in dielectric/ferroelectric layered perovskites: from bulk 3D systems to 2D nanosheets. Dalton Transactions, 2018, 47, 2841-2851.	1.6	42
39	Crystallization and nanometric heterogeneity in glass: <i>In situ</i> observation of the boson peak during crystallization. Physical Review B, 2009, 79, .	1.1	41
40	Controlled doping of semiconducting titania nanosheets for tailored spinelectronic materials. Nanoscale, 2014, 6, 14227-14236.	2.8	41
41	Nanosheet architectonics: a hierarchically structured assembly for tailored fusion materials. Polymer Journal, 2015, 47, 89-98.	1.3	40
42	Mechanical force involved multiple fields switching of both local ferroelectric and magnetic domain in a Bi5Ti3FeO15 thin film. NPG Asia Materials, 2017, 9, e349-e349.	3.8	37
43	Low-Temperature Synthesis of NaNbO3 Nanopowders and their Thin Films from a Novel Carbon-Free Precursor. Journal of the American Ceramic Society, 2006, 89, 1188-1192.	1.9	30
44	Langmuir–Blodgett Fabrication of Nanosheet-Based Dielectric Films without an Interfacial Dead Layer. Japanese Journal of Applied Physics, 2008, 47, 7556.	0.8	30
45	Extra‣arge Mechanical Anisotropy of a Hydrogel with Maximized Electrostatic Repulsion between Cofacially Aligned 2D Electrolytes. Angewandte Chemie - International Edition, 2018, 57, 12508-12513.	7.2	30
46	Single Droplet Assembly for Two-Dimensional Nanosheet Tiling. ACS Nano, 2020, 14, 15216-15226.	7.3	29
47	On/Off Boundary of Photocatalytic Activity between Single- and Bilayer MoS <sub>2</sub> . ACS Nano, 2020, 14, 6663-6672.	7.3	29
48	<i>A</i> ―and <i>B</i> â€6ite Modified Perovskite Nanosheets and Their Integrations into Highâ€ <i>k</i> Dielectric Thin Films. International Journal of Applied Ceramic Technology, 2012, 9, 29-36.	1.1	28
49	Synthesis of Highly Strained Mesostructured SrTiO <sub>3</sub> /BaTiO <sub>3</sub> Composite Films with Robust Ferroelectricity. Chemistry - A European Journal, 2013, 19, 4446-4450.	1.7	27
50	The effects of neodymium content and site occupancy on spontaneous polarization of epitaxial (Bi4â^'xNdx)Ti3O12 films. Journal of Applied Physics, 2005, 98, 024110.	1.1	26
51	Impact of perovskite layer stacking on dielectric responses in KCa2Nanâ^'3NbnO3n+1â€^(n=3–6) Dion–Jacobson homologous series. Applied Physics Letters, 2010, 96, .	1.5	26
52	Precursive stage of nanocrystallization in niobium oxide-containing glass. Applied Physics Letters, 2009, 95, .	1.5	23
53	Hunting for Monolayer Oxide Nanosheets and Their Architectures. Scientific Reports, 2016, 6, 19402.	1.6	23
54	Elucidation of structure and conduction mechanism in Nd-Mn substituted Y-type strontium hexaferrites. Journal of Alloys and Compounds, 2017, 723, 9-16.	2.8	22

#	Article	IF	CITATIONS
55	Probing intrinsic polarization properties in bismuth-layered ferroelectric films. Applied Physics Letters, 2007, 90, 112914.	1.5	21
56	Structural heterogeneity and homogeneous nucleation of 1BaO-2SiO2 glass. Applied Physics Letters, 2009, 94, 211907.	1.5	21
57	Tunable and highly reproducible surface-enhanced Raman scattering substrates made from large-scale nanoparticle arrays based on periodically poled LiNbO3templates. Science and Technology of Advanced Materials, 2013, 14, 055011.	2.8	20
58	<i>In situ</i> Raman spectroscopy for characterization of the domain contributions to electrical and piezoelectric responses in Pb(Zr,Ti)O3 films. Applied Physics Letters, 2010, 97, .	1.5	19
59	2D Inorganic Nanosheets: Twoâ€Dimensional Dielectric Nanosheets: Novel Nanoelectronics From Nanocrystal Building Blocks (Adv. Mater. 2/2012). Advanced Materials, 2012, 24, 209-209.	11.1	17
60	Mn-doped LiNaGe <sub>4</sub> 0 <sub>9</sub> as a rare-earth free phosphor: impact of Na-substitution on emission in tetragermanate phase. Journal of the Ceramic Society of Japan, 2015, 123, 888-891.	0.5	17
61	Highly (0001)-oriented Al-doped ZnO polycrystalline films on amorphous glass substrates. Journal of Applied Physics, 2016, 120, 125302.	1.1	17
62	Multifield Control of Domains in a Room-Temperature Multiferroic 0.85BiTi <sub>0.1</sub> Fe <sub>0.8</sub> Mg <sub>0.1</sub> O <sub>3</sub> –0.15CaTiO <sub>3</sub> Thin Film. ACS Applied Materials & Interfaces, 2018, 10, 20712-20719.	4.0	17
63	Softer region at boundary of supercooled liquid–crystal in glassy fresnoite. Applied Physics Letters, 2009, 94, 241909.	1.5	16
64	A-Site-Modified Perovskite Nanosheets and Their Integration into High-κ Dielectric Thin Films with a Clean Interface. Japanese Journal of Applied Physics, 2010, 49, 09MA01.	0.8	16
65	Design of crystal structures, morphologies and functionalities of titanium oxide using water-soluble complexes and molecular control agents. Polymer Journal, 2015, 47, 78-83.	1.3	16
66	Nitrogen doped ultrathin calcium/sodium niobate perovskite nanosheets for photocatalytic water oxidation. Solar Energy Materials and Solar Cells, 2020, 205, 110283.	3.0	16
67	Solution-Based Fabrication of Perovskite Nanosheet Films and Their Dielectric Properties. Japanese Journal of Applied Physics, 2009, 48, 09KA15.	0.8	15
68	Low-frequency Raman scattering in binary silicate glass: Boson peak frequency and its general expression. Journal of the Ceramic Society of Japan, 2013, 121, 1012-1014.	0.5	15
69	Ferroelectric-assisted gold nanoparticles array for centimeter-scale highly reproducible SERS substrates. Scientific Reports, 2017, 7, 3630.	1.6	15
70	Solution-Processed Two-Dimensional Metal Oxide Anticorrosion Nanocoating. Nano Letters, 2021, 21, 7044-7049.	4.5	15
71	Transmission electron microscopy and <i>in situ</i> Raman studies of glassy sanbornite: An insight into nucleation trend and its relation to structural variation. Journal of Applied Physics, 2010, 108, .	1.1	14
72	Chemical Preparation of Ferroelectric Mesoporous Barium Titanate Thin Films: Drastic Enhancement of Curie Temperature Induced by Mesoporeâ€Đerived Strain. Chemistry - A European Journal, 2014, 20, 11283-11286.	1.7	14

#	Article	IF	CITATIONS
73	Artificial design for new ferroelectrics using nanosheet-architectonics concept. Nanotechnology, 2015, 26, 244001.	1.3	14
74	Layer-by-layer engineering of two-dimensional perovskite nanosheets for tailored microwave dielectrics. Applied Physics Express, 2017, 10, 091501.	1,1	14
75	Tunable Chemical Coupling in Two-Dimensional van der Waals Electrostatic Heterostructures. ACS Nano, 2019, 13, 11214-11223.	7.3	13
76	X-ray nanospectroscopic characterization of a molecularly thin ferromagnetic Ti1â^'xCoxO2 nanosheet. Applied Physics Letters, 2008, 93, 093112.	1.5	12
77	Realization of graphene field-effect transistor with high-κ HCa2Nb3O10 nanoflake as top-gate dielectric. Applied Physics Letters, 2013, 103, .	1.5	12
78	Scalable Design of Twoâ€Dimensional Oxide Nanosheets for Construction of Ultrathin Multilayer Nanocapacitor. Small, 2020, 16, 2003485.	5.2	12
79	Rational Assembly of Two-Dimensional Perovskite Nanosheets as Building Blocks for New Ferroelectrics. ACS Applied Materials & Interfaces, 2021, 13, 1783-1790.	4.0	12
80	Construction of Multilayer Films and Superlattice- and Mosaic-like Heterostructures of 2D Metal Oxide Nanosheets via a Facile Spin-Coating Process. ACS Applied Materials & Interfaces, 2021, 13, 43258-43265.	4.0	12
81	Solution-Based Fabrication of Perovskite Multilayers and Superlattices Using Nanosheet Process. Japanese Journal of Applied Physics, 2011, 50, 09NA10.	0.8	12
82	Enhanced dielectric response induced by controlled morphology in rutile TiO <sub>2</sub> nanocrystals. Journal of the Ceramic Society of Japan, 2013, 121, 593-597.	0.5	11
83	Origin of Extended UV Stability of 2D Atomic Layer Titania-Based Perovskite Solar Cells Unveiled by Ultrafast Spectroscopy. ACS Applied Materials & Interfaces, 2019, 11, 21473-21480.	4.0	11
84	Synthesis of NaMoO3F and Na5W3O9F5 with Morphological Controllability in Non-Aqueous Solvents. Inorganic Chemistry, 2020, 59, 10707-10716.	1.9	11
85	Hydration of Sodium Cobalt Oxide. Chemistry of Materials, 2007, 19, 6073-6076.	3.2	10
86	Crystallization of tungstenbronze-type Ba2NaNb5O15 in high-Nb2O5-content glass: An inelastic light scattering study. Journal of Applied Physics, 2010, 108, 103519.	1.1	10
87	Observation of ferroelectric domains in bismuth-layer-structured ferroelectrics using Raman spectroscopy. Materials Science and Engineering B: Solid-State Materials for Advanced Technology, 2005, 120, 95-99.	1.7	9
88	Solution-Based Fabrication of High-κ Dielectric Nanofilms Using Titania Nanosheets as a Building Block. Japanese Journal of Applied Physics, 2007, 46, 6979.	0.8	9
89	Formation of spherulite and metastable phase in stoichiometric Ba2Si3O8 glass. Journal of the Ceramic Society of Japan, 2010, 118, 955-958.	0.5	9
90	Gigantic plasmon resonance effects on magneto-optical activity of molecularly thin ferromagnets near gold surfaces. Journal of Materials Chemistry C, 2013, 1, 2520.	2.7	9

#	Article	IF	CITATIONS
91	Successive phase transformation in stoichiometric glassy Li2Ge4O9: Isothermal and nonisothermal study. Journal of Applied Physics, 2013, 114, .	1.1	9
92	Single crystal-like selection rules for unipolar-axis oriented tetragonal Pb(Zr,Ti)O3 thick epitaxial films. Applied Physics Letters, 2010, 97, 111901.	1.5	8
93	Soft-phonon mode observation in Li2Ge4O9 phase above room temperature. Applied Physics Letters, 2012, 100, 091902.	1.5	8
94	High-temperature dielectric responses of molecularly-thin titania nanosheet. Journal of the Ceramic Society of Japan, 2015, 123, 335-339.	0.5	8
95	Thermally stable dielectric responses in uniaxially (001)-oriented CaBi4Ti4O15 nanofilms grown on a Ca2Nb3O10â^ nanosheet seed layer. Scientific Reports, 2016, 6, 20713.	1.6	8
96	High-temperature dielectric responses in all-nanosheet capacitors. Japanese Journal of Applied Physics, 2017, 56, 06GH09.	0.8	8
97	Crystallization and Morphology of Glassy Sanbornite. Key Engineering Materials, 0, 485, 301-304.	0.4	7
98	Oriented Film Growth of Ba <sub>1–<i>x</i></sub> Sr <sub><i>x</i></sub> TiO <sub>3</sub> Dielectrics on Glass Substrates Using 2D Nanosheet Seed Layer. ACS Applied Materials & Interfaces, 2013, 5, 4592-4596.	4.0	7
99	Oxygen vacancies in PbTiO <sub>3</sub> thin films probed by resonant Raman spectroscopy. Journal of the Ceramic Society of Japan, 2013, 121, 598-601.	0.5	7
100	Advanced capacitor technology based on two-dimensional nanosheets. Japanese Journal of Applied Physics, 2016, 55, 1102A3.	0.8	7
101	Enhanced oxide-ion conductivity of solid-state electrolyte mesocrystals. Nanoscale, 2019, 11, 4523-4530.	2.8	7
102	Resonant two-phonon Raman scattering as a probe of hole crystal formation inSr14â^'xCaxCu24O41. Physical Review B, 2006, 74, .	1.1	6
103	Nanoscale Characterization of Domain Structures in Bi\$_{4}\$Ti\$_{3}\$O\$_{12}\$ Single Crystals Using Near-Field Raman Spectroscopy. Japanese Journal of Applied Physics, 2011, 50, 09NE10.	0.8	6
104	Solution-Based Fabrication of Perovskite Multilayers and Superlattices Using Nanosheet Process. Japanese Journal of Applied Physics, 2011, 50, 09NA10.	0.8	6
105	Origin of thermally stable ferroelectricity in a porous barium titanate thin film synthesized through block copolymer templating. APL Materials, 2017, 5, .	2.2	6
106	Chemical Synthesis of Porous Barium Titanate Thin Film and Thermal Stabilization of Ferroelectric Phase by Porosity-Induced Strain. Journal of Visualized Experiments, 2018, , .	0.2	6
107	(Invited) New Dielectric Nanomaterials Fabricated from Nanosheet Technique. ECS Transactions, 2012, 45, 3-8.	0.3	5
108	Investigation of PbTiO <sub>3</sub> thin films with reduced and re-oxidized treatment using Raman spectroscopy. Journal of the Ceramic Society of Japan, 2013, 121, 859-862.	0.5	5

MINORU OSADA

#	Article	IF	CITATIONS
109	Self-Sensitization and Photo-Polymerization of Diacetylene Molecules Self-Assembled on a Hexagonal-Boron Nitride Nanosheet. Polymers, 2018, 10, 206.	2.0	5
110	Impacts of intrinsic defects on luminescence properties of CuAlS2. Applied Physics Letters, 2006, 89, 221117.	1.5	4
111	Low-frequency inelastic light scattering of zincogermanate glass in supercooledliquid regime. Journal of Applied Physics, 2011, 109, 126105.	1.1	4
112	Effect of annealing at maximum nucleation temperature on boson peak in lithium-disilicate glass. Journal of the Ceramic Society of Japan, 2012, 120, 256-258.	0.5	4
113	NANOCRYSTALLIZATION AND OPTICAL PROPERTY OF WILLEMITE-TYPE SEMICONDUCTIVE Zn2GeO4 IN GLASS. Functional Materials Letters, 2012, 05, 1260008.	0.7	4
114	Spectroscopically and thermometrically observed boson peaks in oxide glass system. Japanese Journal of Applied Physics, 2015, 54, 088003.	0.8	4
115	Synthesis of green emission upconversion phosphor nanosheets (LaNb2O7) doped with Er3+ and Yb3+. Journal of Luminescence, 2016, 173, 130-134.	1.5	3
116	Magneto-Optical Effects in Superlattice Assemblies of Ferromagnetic Nanosheets. Key Engineering Materials, 2007, 350, 15-18.	0.4	2
117	Polarized Raman Study for Epitaxial PZT Thick Film with the Mixture Orientation of (100)/(001). Key Engineering Materials, 0, 421-422, 99-102.	0.4	2
118	Inelastic light scattering from nanocrystallizing niobiotellurite glass: an insight into the metastable phase and phase-transformation dynamics. Journal of the Ceramic Society of Japan, 2010, 118, 814-818.	0.5	2
119	Chemical Nanomanipulation of Two-Dimensional Nanosheets and Its Applications. , 0, , .		2
120	Fabrication and Properties of Microcapacitors with a One-nanometer-thick Single Ti0.87O2 Nanosheet. Chemistry Letters, 2014, 43, 307-309.	0.7	2
121	Facile titania nanocoating using single droplet assembly of 2D nanosheets. Journal of the Ceramic Society of Japan, 2021, 129, 359-364.	0.5	2
122	Nanoscale Characterization of Domain Structures in Bi4Ti3O12Single Crystals Using Near-Field Raman Spectroscopy. Japanese Journal of Applied Physics, 2011, 50, 09NE10.	0.8	2
123	Antiferromagnetic Ordering Coupled with Phonon Mode Anomalies in Rare-Earth Cuprate NdCu2O4, Probed by Nuclear Quadrupole Resonance and Raman Spectroscopy. Journal of the Physical Society of Japan, 2005, 74, 2076-2081.	0.7	1
124	Nanoâ€Materials Design for Highâ€ <i>T</i> <sub>C</sub> Ferromagnets of <scp><scp>Ti<sub>1â€x</sub>Co<sub>x</sub>O<sub>2</sub></scp></scp> Nanosheets. International Journal of Applied Ceramic Technology, 2012, 9, 936-941.	1.1	1
125	Identification of the Occupation Site of Dy- or Y-Substituted PZT Films and the Correlation Between Occupation Site and Ferroelectric Property. Integrated Ferroelectrics, 2013, 141, 1-8.	0.3	1
126	Transmission electron microscopy and in situ Raman studies of glassy sanbornite: An insight into nucleation trend and its relation to structural variation. , 0, .		1

8

MINORU OSADA

#	Article	IF	CITATIONS
127	New Perovskite Nanomaterials and Their Integrations into High-k Dielectrics. Additional Conferences (Device Packaging HiTEC HiTEN & CICMT), 2011, 2011, 000072-000077.	0.2	1
128	Strategic Smart Process for the Fabrication of Ultimate Functional ZnO Materials with Highly Transparent Conductivity. Journal of Smart Processing, 2013, 2, 236-244.	0.0	1
129	The Effect of Varying Ca-Content on the Structure of High-T <sub>c</sub> Superconductor (Ca <sub>x</sub> La <sub>1-x</sub> )(Ba <sub>1.75-x</sub> La <sub>0.25+x&lt; (x = 0.5, 0.6, and 0.8) Studied by Neutron Powder Diffraction. Materials Science Forum, 2004, 443-444, 361-364.</sub>	t;/sub>) 0.3	Cu <sub< td=""></sub<>
130	Phase Control in High-Temperature Superconductors and Novel Fabrication Procedure for Superconducting Components. Key Engineering Materials, 2004, 269, 91-94.	0.4	0
131	Self Assemble Synthesis of Potassium Niobate at Room Temperature. Key Engineering Materials, 2006, 320, 7-10.	0.4	0
132	Photoconducting Properties in Oxygen-Deficient Bi <sub>4</sub> Ti <sub>3</sub> O <sub>12</sub> . Key Engineering Materials, 2006, 301, 7-10.	0.4	0
133	Exciton-Phonon Interaction in CuAlS <sub>2</sub> Powders. Advanced Materials Research, 2006, 11-12, 175-178.	0.3	ο
134	Photoinduced Nanodots in Bi <sub>2</sub> Sr <sub>2</sub> CaCu <sub>2</sub> O <sub>8+d</sub> . Key Engineering Materials, 2006, 320, 167-170.	0.4	0
135	Synthesis of Complex Perovskite Oxides via Nanosheets Process. Key Engineering Materials, 2007, 350, 55-58.	0.4	0
136	Ferromagnetic Properties in Co-Substituted Titania Nanosheets. Key Engineering Materials, 2008, 388, 119-122.	0.4	0
137	Investigation of Oxygen Vacancies in Micro-Patterned PZT Thin Films Using Raman Spectroscopy. Key Engineering Materials, 2009, 421-422, 135-138.	0.4	ο
138	Focus on innovation in ceramics research in East Asia. Science and Technology of Advanced Materials, 2010, 11, 040301.	2.8	0
139	Low-Frequency Inelastic Light Scattering of Glassy Ba <sub>2</sub> TiGe <sub>2</sub> O <sub>8</sub> during Heating Process. Key Engineering Materials, 0, 445, 225-228.	0.4	0
140	Fabrication of Artificial Superlattices Using Perovskite Nanosheets. Key Engineering Materials, 2011, 485, 321-324.	0.4	0
141	Self-assembly of oxide nanosheets: precise structural control and its applications. , 2012, , 618-620.		0
142	Crystallization of Tungstenbronze Phase and its Inelastic Light Scattering in Niobiophosphate-System Glass. Key Engineering Materials, 0, 566, 306-309.	0.4	0
143	Nanosheet-Based Electronics. Nanostructure Science and Technology, 2017, , 347-356.	0.1	0
144	Self-Assembly of Oxide Nanosheets: Precise Structural Control and Its Applications. , 2018, , 797-799.		0

#	Article	IF	CITATIONS
145	Atomic Layer Technology Based on 2D Inorganic Nanosheets. Materia Japan, 2021, 60, 628-633.	0.1	ο
146	Structures and Physical Properties in Oxide Nanosheets. Nihon Kessho Gakkaishi, 2012, 54, 352-358.	0.0	0
147	Nanosheet Coating Process. Yosetsu Gakkai Shi/Journal of the Japan Welding Society, 2014, 83, 95-99.	0.0	Ο
148	Controlled Assembly of Inorganic Nanosheets and Its Application to High-Performance Metamaterials. Hyomen Gijutsu/Journal of the Surface Finishing Society of Japan, 2019, 70, 355-358.	0.1	0